# MESH REFINEMENT BASED ON THE 8-TETRAHEDRA LONGEST-EDGE PARTITION

Ángel Plaza[1] María-Cecilia Rivara[2]

[1] *University of Las Palmas de Gran Canaria, Spain, aplaza@dmat.ulpgc.es*
[2] *DCC, University of Chile, Santiago de Chile, Chile, mcrivara@dcc.uchile.cl*

## ABSTRACT

The 8-tetrahedra longest-edge (8T-LE) partition of any tetrahedron is defined in terms of three consecutive edge bisections, the first one performed by the longest-edge. The associated local refinement algorithm can be described in terms of the polyhedron skeleton concept using either a set of precomputed partition patterns or by a simple edge-midpoint tetrahedron bisection procedure. An effective 3D derefinement algorithm can be also simply stated. In this paper we discuss the 8-tetrahedra partition, the refinement algorithm and its properties, including a non-degeneracy fractal property. Empirical experiments show that the 3D partition has analogous behavior to the 2D case in the sense that after the first refinement level, a clear monotonic improvement behavior holds. For some tetrahedra a limited decreasing of the tetrahedron quality can be observed in the first partition due to the introduction of a new face which reflects a local feature size related with the tetrahedron thickness.

**Keywords: mesh refinement, longest-edge bisection, longest-edge algorithms, tetrahedral meshes**

## 1. INTRODUCTION

Skeleton algorithms for local mesh refinement /derefinement of triangular and tetrahedral meshes have been proposed by Plaza and Carey [10, 11, 12]. In two dimensions, the algorithm is an alternative formulation of the 4-triangles longest-edge algorithm [14, 15]. The 2-dimensional skeleton algorithm [10, 11] works over the edges wireframe mesh affected by the refinement (target triangles and some neighbors to assure the construction of a conforming mesh) by performing midpoint bisection of the involved edges. Then this information is used to select the appropriate triangle partition pattern (between a set of three patterns) to refine each individual triangle. This idea was then generalized to 3-dimensions [11, 12] by introducing an 8-tetrahedra partition which induces the 4-triangles partition of its faces.

The 3-dimensional skeleton algorithm performs: (1) the refinement of the 3-dimensional edges wireframe mesh affected, (2) the refinement of the faces surface mesh (by using the 4-triangles partition and associated partial partitions), and (3) the volume refinement of each tetrahedron either by using a simple edge bisection procedure or according to an appropriate pattern, selected between a set of precomputed partition patterns.

In this paper we study the properties of the 8-tetrahedra partition showing that each full partition pattern is equivalent to a sequence of seven tetrahedron edge bisections by the midpoint of the tetrahedron edges, the first one being performed by the tetrahedron longest-edge. Then we take advantage from the improvement and fractal properties of the 4-triangles longest-edge partition to show some non-degeneracy properties in 3-dimensions. We also show that for the meshes globally refined by using the 8-tetrahedra partition, the asymptotic average number of tetrahedra sharing a fixed vertex is equal to 24.

An empirical study about the behavior of the 8-tetrahedra partition is also included. This shows that consistently, from the second refinement level, both

the distribution of quality tetrahedra, and the volume percentage covered by better tetrahedra tend to be improved as the 8T-LE partition proceeds.

### 1.1 Previous and related work

Refinement algorithms based on longest-edge partitions, including Lepp based algorithms, have been extensively discussed [14, 15, 18, 17, 16], as well as skeleton based algorithms [10, 11, 12, 13].

In two-dimensions it has been shown that these algorithms improve the point distribution by maintaining some small-angled triangles which depend on the quality of the initial mesh, in the following senses: the iterative global refinement of any triangle produces triangles whose minimum angle is bounded as a function of the quality of the initial triangle, the process produces a finite number of similarly distinct triangles, and both the percentage of good-quality triangles and the area covered by these triangles increases as the refinement proceeds.

In [18] a pure three dimensional longest-edge refinement method was considered. Empirical experimentation showing that the solid angle decreases slowly with the refinement iterations and that a quality-element improvement behavior, analogous to the 2-dimensional case holds in practice, were provided. However, there has not been mathematical results available guaranteeing the non-degeneracy properties of the 3-dimensional mesh.

In the last 12 years other triangle-bisection and tetrahedron-bisection refinement algorithms have been proposed. Between them we can cite the newest-vertex insertion method of Michell [9] in two dimensions, the tetrahedron-bisection algorithm of Bänsch [2] and the 8-tetrahedra bisection algorithm of Liu and Joe [7]. These algorithms essentially consist on performing edge based partitions in such a way that triangles or tetrahedra similar to those of the first refinement levels are obtained throughout the process. In particular, Liu and Joe have obtained a bound on the mesh quality as a function of the initial geometry for their algorithm [6].

Other studies report somewhat equivalent algorithms. A recursive approach which imposes certain restrictions and pre-processing in the initial mesh is proposed by Kossaczký [4]. Maubach [8] has developed and algorithm for $n$-simplicial grids generated by reflection. Although the algorithm is valid in any dimension and the number of similarity classes is bounded, this cannot be applied to a general tetrahedral grid, since an additional closure refinement is needed to avoid incompatibilities. Arnold *et al.* [1] have presented an algorithm equivalent to those discussed in [2, 4] proving its equivalence with [8].

All these algorithms however, do not take practical advantage of the element-quality improvement properties of longest-edge and skeleton algorithms. These algorithms, in exchange, can be applied to any valid initial triangulation without any restriction on the shape of the tetrahedra.

In what follows we specifically discuss the skeleton algorithms of Plaza and Carey [10, 11, 12]. This three dimensional approach is based on the application of the 2-dimensional algorithm over the skeleton of the 3D triangulation, that is to the set of the triangular faces of the tetrahedra. Being this a longest-edge based algorithm we expect for it analogous behavior to that reported in [18] for pure 3-dimensional longest-edge refinement algorithm.

## 2. THE 4-TRIANGLES ALGORITHM AND PREVIOUS RESULTS

The 4-Triangles algorithm can be described in terms of the three refinement patterns of Figure 1, where $P$ is the midpoint of the longest-edge. The algorithm consists on two basic steps: (1) refinement of target triangles by using the partition pattern (a) of Figure 1, and (2) a local propagation step to assure a conforming mesh which uses the partition patterns of (b) and (c) of Figure 1.

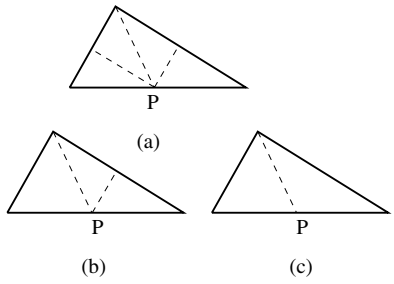


**Figure 1**: 4-Triangles-refinement patterns.

**4-Triangles-Refinement-Algorithm**$(\tau, t)$
/* Perform the 4-Triangles partition of $t$
for each edge $e$ of $t$, of associated neighbor $t^*$ do
    neighbor-refinement$(t^*, e)$
    $t \leftarrow t^*$
    while $t$ is non-conforming do
        find the unique non-conforming edge $e \in t$
            with associated neighbor $t^*$
        neighbor-refinement$(t^*, e)$
        $t \leftarrow t^*$
    end while
end for

neighbor-refinement($t^*, e$)
if $e$ is longest-edge of $t^*$ perform LE bisection of $t^*$
else perform 3-Triangles partition of $t^*$ by edge $e$

For an illustration see Figure 2. Note that in the general case, the refinement should propagate to neighbor triangles by the edges $AC$ and $CB$.

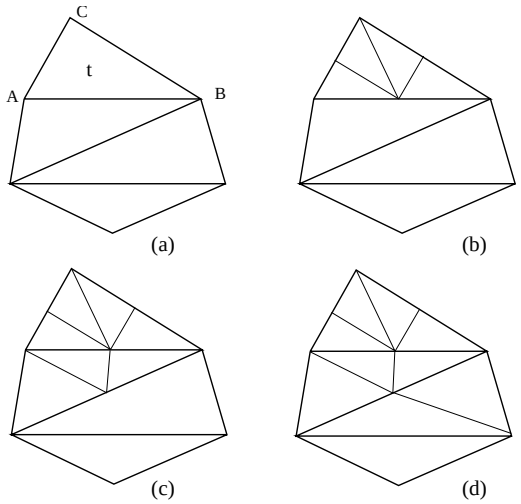


**Figure 2**: Example of 4-Triangles-Refinement-Algorithm.

The 4-Triangles-Algorithm produces a subset of the triangles obtained by longest-edge bisection and the following theorem holds [14, 15]:

**Theorem 2.1** *Over any conforming triangulation $\tau_0$, the iterative application of the 4-Triangles-Algorithm: (1) produces nested triangulations in the sense that each new triangle is embedded in its parent; (2) every triangle $t$ generated in the process has smallest angle greater or equal to $\frac{\alpha_0}{2}$, where $\alpha_0$ is the smallest angle of the triangle $t_0$ in $\tau$ which embeds $t$; (3) produces a finite number of similarity distinct triangles; (4) the triangulations obtained tend to be improved in the sense that both the percentage of the good-quality triangles and the area covered by these triangles increases as the refinement proceeds.*

Furthermore, for obtuse triangles the following monotone improvement behavior holds [17]:

**Theorem 2.2** *For any obtuse triangle $t_0$ of smallest angle $\alpha_0$ and largest angle $\gamma_0$, the 4-Triangles partition of $t_0$ produces a unique similarly distinct triangle $t_1$, whose 4-Triangles partition in turn produces a new similarly distinct triangle $t_2$, and so on, until a last non-obtuse triangle $t_n$ is obtained. Furthermore, the smallest angles $\alpha_i$ and the largest angles $\gamma_i$ of each triangle $t_i$ satisfy the following improvement relations:*

$$\alpha_0 < \alpha_1 < \alpha_2 < \ldots < \alpha_n$$
$$\gamma_0 > \gamma_1 > \gamma_2 > \ldots > \gamma_n$$

*where $\gamma_i = \gamma_{i-1} - \alpha_i$.*

For the 4T-LE algorithm, a fractal property analogous to that proved for the LE-bisection algorithm [17] also holds:

**Theorem 2.3** *After a finite number of iterative (local) applications of the 4-triangles algorithm around any vertex $P$ of any conforming triangulation $\tau$, a stable molecule around $P$ is obtained, in the sense that the next iteration of the algorithm do not divide the angles of vertex $P$, but only introduce new vertices along the edges of the stable molecule. Furthermore, each new triangle of vertex $P$ produced throughout the next iterations will be similarly equal to a preceding triangle.*

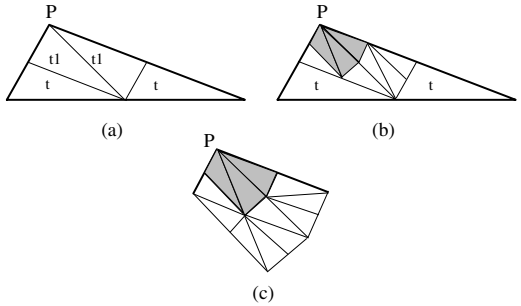


**Figure 3**: Fractal behavior of 4-triangles partition and stable molecule.

## 2.1 The skeleton algorithms in two and three dimensions

The skeleton version of the 4-Triangles refinement algorithm performs the refinement task by using two sequential steps: (1) Identifying and bisecting the edges (not the triangles) involved throughout the overall refinement process; and (2) partitioning each individual triangle involved in the refinement process by using the triangles partitions of Figure 1 according to its bisected edges.

The 3D-skeleton algorithm in exchange generalizes the 4-Triangles refinement algorithm to 3-dimensions by

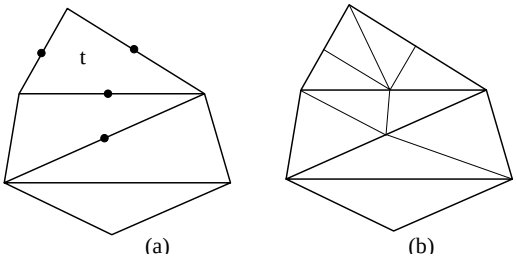


**Figure 4**: Example of the use of the 2D-skeleton algorithm.

making use of the skeleton concept which in turn generalizes the graph usually associated with the polygonal faces of any polyhedron [10, 11, 3]:

**Definition 2.4** *For any conforming 3D triangular mesh $\tau$ (tetrahedral mesh), the 2D-Skeleton of $\tau$ is the conforming surface mesh defined by the triangular faces of the elements of $\tau$. In addition, the 1D-Skeleton of $\tau$ is the conforming wire mesh defined by the edges of the elements of $\tau$.*

By using the preceding concepts the algorithm can be schematically described as follows:

**3D-Skeleton Refinement-Algorithm**$(\tau, t)$
Find and Partition involved Edges over
1-skeleton mesh
Partition involved Faces over 2-skeleton mesh
Partition involved Tetrahedra according
appropriate partition patterns

Note that with minor changes, both procedures (over the 1-skeleton mesh and the 2-skeleton mesh) together correspond to the application of the 4-Triangles-Skeleton-Refinement Algorithm to the surface triangulation formed by the faces of the tetrahedra of the initial 3-dimensional triangulation. The Partition Tetrahedra procedure in exchange performs the volume partition of the set of tetrahedra whose faces were refined by the preceding procedures.

In the next Section we shall introduce and discuss the 8-Tetrahedra-LE partition, proving the following properties: the 8-tetrahedra LE partition of every tetrahedron $t$ in the mesh produces both a conforming volume mesh and a conforming surface mesh where the surface mesh is obtained by the 4-Triangles partition of the faces of t.

## 3. THE 8-TETRAHEDRA PARTITION AND PROPERTIES

At this point, some definitions are in order:

**Definition 3.1** *For any tetrahedron $t$ of unique longest-edge, the primary faces of $t$ are the two faces of $t$ that share the longest-edge of $t$. In addition, the two remaining faces of $t$ are called secondary faces of $t$. Furthermore, the secondary edges of $t$ are the longest edges of the secondary faces of $t$ (1 or 2 secondary longest edges). In addition, the 3 or 4 remaining edges of $t$ are called third-class edges of $t$.*

Note that for any tetrahedron $t$ of unique longest-edge, the primary faces of $t$ have a common longest-edge equal to the longest-edge of $t$. In order to avoid ambiguousness in the general case, we always suppose that for each tetrahedron $t$ having either a non-unique longest-edge, or non-unique secondary edges, a unique selection for each of such edges is performed a priori in such a way that the longest-edge of the tetrahedron coincides with the longest-edge of the primary faces of $t$, and this selection is consistently maintained throughout the overall refinement process.

The 8-Tetrahedra longest-edge partition can be defined as follows:

**Definition 3.2** *For any tetrahedron $t$ of unique longest-edge and unique secondary edges, the 8-Tetrahedra Longest-Edge (8T-LE) partition of $t$ is defined as follows:*

*(1) LE-bisection of $t$ producing tetrahedra $t_1, t_2$;*
*(2) bisection of $t_i$ by the midpoint of the unique edge of $t_i$ which is also a secondary edge of $t$, producing tetrahedra $t_{ij}$ for $i, j = 1, 2$.*
*(3) bisection of each $t_{ij}$ by the midpoint of the unique edge equal to a third-class edge of $t$, for $i, j = 1, 2$.*

In order to study the 8-tetrahedra partition, we need to consider an intermediate 4-tetrahedra partition characterized by the following proposition:

**Proposition 3.3** *Let $t$ be any tetrahedron of unique longest-edge $AB$ and associated midpoint $P$ (see Figure 5. Then the 4-tetrahedra partition described by the two ordered steps (1) and (2) of Definition (3.2) produces a 4-tetrahedra volume triangulation of $t$ satisfying the following properties:*

*a) The volume triangulation induces the longestedge bisection of each triangular face of $t$.*
*b) The volume triangulation of $t$ will be a conforming triangulation if and only if the distribution of the longest-edge and secondary edges of $t$ corresponds to either the cases (a), (b), or (c) in Figure 5.*
*c) The volume triangulation will not be a conforming triangulation if and only if the secondary edges share a vertex and one of these edges is opposite to the longest-edge of $t$ (Figure 5 (d)).*

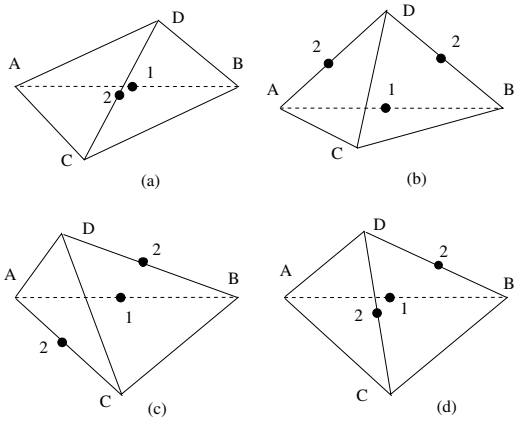


**Figure 5**: Relative position of the longest-edge (numbered 1) and secondary longest-edges (numbered 2) for $t$.

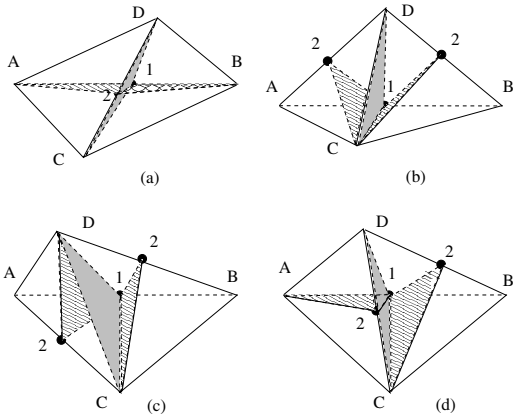


**Figure 6**: 4-Tetrahedron partition obtained according to the relative positions of the longest-edge and secondary longest-edges of $t$.

The proof of part a) follows directly from the definition of the 4-tetrahedra partition, while the proof of parts b) and c) are based on the study of the possible relative positions of the longest-edge of $t$ and the secondary edges of $t$. Clearly, only 4 relative configurations, invariant under translation, rotation, reflection and uniform scaling are possible:

i) longest-edge of $t$ opposite to the unique (common) secondary edge of the two secondary faces of $t$ (Figure 5 (a)).

ii) the secondary longest-edges and longest-edge of $t$ form a triangular face of $t$ (Figure 5 (b)).

iii) opposite secondary edges, where each of such edges shares a vertex with the longest-edge of $t$ (Figure 5 (c)).

iv) the secondary edges share a vertex and one of the secondary edges is opposite to the longest-edge of $t$ (Figure 5 (d)).

**Corollary 3.4** *The 4-tetrahedra partition of Theorem 3.3 produces four tetrahedra $t_{ij}$ for $i, j = 1, 2$ such that each $t_{ij}$ has a unique edge equal to a third-class edge of $t$.*

The next proposition proves that, for the 4 cases of Proposition 3.3 (Figure 6), the midpoint edge bisection of the new tetrahedra (by the non-bisected edge of $t$) produces a conforming volume triangulation of $t$.

**Proposition 3.5** *Let $t$ be any tetrahedron having a unique longest-edge and unique secondary edges. Then if after applying the 4-tetrahedra partition defined in Proposition 3.3, each of the tetrahedra $t_{ij}$ produced by this partition is in turn bisected by the midpoint of the (unique) edge equal to a third-class edge of $t$, a conforming volume triangulation is obtained having the following properties:*

*a) The volume triangulation induces the 4-triangles partition of each face of $t$.*

*b) Only an interior edge $P^*P$ is produced, where $P$ and $P^*$ are respectively the midpoint of the longest-edge of $t$, and the midpoint of the edge opposite to the longest-edge of $t$.*

*c) Eight new internal faces appear inside the tetrahedron $t$.*

The results of previous proposition allow us to state Theorem 3.6:

**Theorem 3.6** *The 8-tetrahedra longest-edge partition of any tetrahedron $t$ produces both a conforming volume triangulation of $t$ and a conforming surface triangulation of $t$ such that:*

*(1) The conforming surface triangulation of $t$ is identical to the surface triangulation obtained by the 4-triangles partition of the faces of $t$.*

*(2) Four different triangulation patterns are obtained (Figure 7) according with the relative position of the longest-edge and the secondary edges of $t$. Each one of these 4 patterns produces only one new internal edge $P^*P$ (where $P$ is the midpoint of the longest-edge of $t$, and $P^*$ is the midpoint of the edge opposite to the longest-edge) and 8 new internal faces.*

Note that under the assumption that the longest-edge and the secondary edges are unique, there is a univocal correspondence between the four volume partition

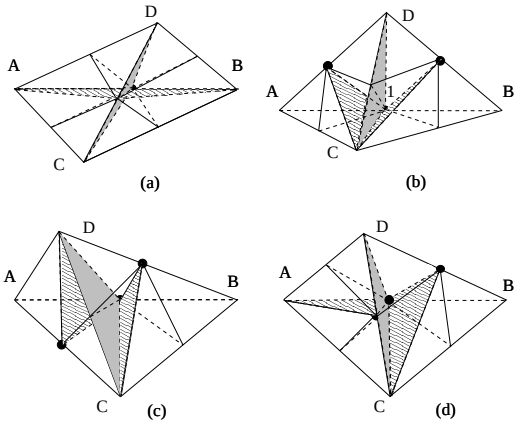


**Figure 7**: Different possible 8-Tetrahedra Longest-Edge partitions.

patterns produced by the 8-tetrahedra partition of any tetrahedron $t$ and the four surface partition patterns obtained by the 4-triangles partition of the faces of $t$.

The careful study of the possible $n$-point partition patterns produced for the different relative positions of the longest-edge and secondary edges of $t$, for $n = 1, 2, \ldots, 6$ (which includes the four global 8-tetrahedra partition patterns) allows us to obtain the set of partial partition patterns involved in the mesh refinement algorithm. It can be proved that the are exactly 30 different partition patterns (invariant under translation, rotation, reflection, and uniform scaling) associated to the 8-tetrahedra partition of any tetrahedron.

## 4. THE 3D-SKELETON REFINEMENT/DEREFINEMENT ALGORITHM

The refinement algorithm for refining any tetrahedron $t$ in any conforming tetrahedral mesh $\tau$ can be formulated as follows:

**3D-Skeleton-Refinement-Algorithm**$(\tau, t)$
/* Find involved edges, faces, and tetrahedra */
Initialize $S_E$, $S_F$, and $S_T$, respectively sets of involved edges, faces, and tetrahedra
Initialize $\mathcal{P}_E$ set of processing edges
for each edge $E$ of $t$ do
    add edge $E$ to set $S_E$
    add edge $E$ to set $\mathcal{P}_E$
endfor
While $\mathcal{P}_E \neq \emptyset$, do
    pick $E$ from $\mathcal{P}_E$
    for each tetrahedron $t^\star$ sharing edge $E$ do
        for each face $F$ of $t^\star$ having an edge in $S_E$ do
            find longest-edge $E^\star$ of $F$
            if $E^\star$ is not in $S_E$ do
                add $E^\star$ to $S_E$
                add $E^\star$ to $\mathcal{P}_E$
                add $F$ to $S_F$
            endif
        endfor
        add $t^\star$ to $S_T$
    endfor
Endwhile
/* Partition involved edges */
for each edge $E$ in $S_E$ do
    create vertex $P$ midpoint of $E$
    bisect $E$
endfor
/* Partition involved faces */
for each edge $F$ in $S_F$ do
    partition $F$ according its bisected edges
endfor
/* Partition involved tetrahedra */
for each tetrahedron $T$ in $S_T$ do
    partition $T$ according to the partition of its faces
end for

The 3-dimensional skeleton refinement algorithm generalizes the 2-dimensional 4T-LE algorithm in the following sense:

**Theorem 4.1** *The refined volume mesh obtained by the use of the 3D-Skeleton-Refinement-Algorithm induces the surface refinement of the associated 2D-Skeleton mesh and viceversa. Furthermore, the surface refined mesh is identical to the mesh obtained by applying the 4-triangles mesh refinement to the faces of $t$.*

**Corollary 4.2** *The 3-dimensional skeleton refinement algorithm is finite.*

Note that the tetrahedra partition step can be implemented either by successive application of a basic tetrahedron bisection operation by an edge midpoint, or by precomputing a set of partition patterns. Also, an alternative algorithm working directly with the volume mesh (without using the mesh-skeleton concept) can be developed.

The derefinement algorithm works on the finite sequence of nested meshes obtained by the refinement algorithm application $T = \{\tau_1 < \ldots < \tau_n\}$ to obtain another sequence of meshes. The algorithm essentially comprises two main steps: the application of the 4T-LE derefinement algorithm to the skeleton (working firstly both over the wireframe mesh and the triangular surface mesh), then followed by the

redefinition of the interior of the tetrahedra, for which a slight variation of the 3D refinement algorithm is used. For a further discussion see Plaza *et al.* in [12].

## 5. ON THE NON-DEGENERACY PROPERTIES OF THE 8T-LE REFINEMENT ALGORITHMS

**Theorem 5.1** *Let $\tau_0$ be any initial conforming tetrahedral mesh having a number of vertices, edges, faces, and tetrahedra respectively equal to $N_0$, $E_0$, $F_0$, and $T_0$; and consider the global use of the 3D-Skeleton Mesh Refinement algorithm producing a sequence of globally refined meshes $\tau_1, \tau_2, \ldots, \tau_n, \ldots$ Then the average number of tetrahedra sharing a vertex in the mesh is asymptotically equal to 24, the average number of faces sharing a vertex is asymptotically equal to 24, and the average number of edges per vertex tends to 14.*

The proof is based on the resolution of the recurrence equations associated to the 8-tetrahedra longest-edge partition. Note that the global refinement of each mesh $\tau_{n-1}$ reduces to the 8-tetrahedra longest-edge partition of all the tetrahedra of $\tau_{n-1}$ which directly produces a conforming mesh $\tau_n$. By Theorem 3.6, the number of vertices, edges, faces, and tetrahedra of the mesh $\tau_n$, respectively equal to $N_n$, $E_n$, $F_n$, and $T_n$, satisfy the following recurrence relations as a function of the values $N_{n-1}$, $E_{n-1}$, $F_{n-1}$, and $T_{n-1}$ of the previous mesh:

$$\begin{array}{rcl} N_n & = & N_{n-1} + E_{n-1} + T_{n-1} \\ E_n & = & 2 \cdot E_{n-1} + 3 \cdot F_{n-1} + T_{n-1} \\ F_n & = & 4 \cdot F_{n-1} + 8 \cdot T_{n-1} \\ T_n & = & 8 \cdot T_{n-1} \end{array} \qquad (1)$$

where $N_0$, $E_0$, $F_0$, and $T_0$ are given from the initial mesh $\tau_0$.

Furthermore, since each tetrahedron has exactly four vertices, the average number of tetrahedra sharing a given vertex in the mesh $\tau_n$ reduces to:

$$Av\#(\text{tetrahedra per node}) = \frac{4 \cdot T_n}{N_n}$$

And, in a similar way, the rest of the non-constant adjacency relations are:

$$Av\#(\text{tet per edge}) = \frac{6 \cdot T_n}{E_n}$$

$$Av\#(\text{faces per edge}) = \frac{3 \cdot F_n}{E_n}$$

$$Av\#(\text{faces per node}) = \frac{3 \cdot F_n}{N_n}$$

$$Av\#(\text{edges per node}) = \frac{2 \cdot E_n}{N_n}.$$

Once the recurrence relations (1) are solved, the asymptotic values are obtained taking limits when $n$ tends to infinity. See reference [13] for details.

The following theorem summarizes geometrical and fractal properties of the 8T-LE refinement algorithm.

**Theorem 5.2** *Both for the 8T-LE partition and for the 3D-Skeleton Refinement algorithm the following mesh quality properties hold:*

*a) The 8T-LE partition of any tetrahedron $t$ always partitions the largest planar angles of the two faces sharing the longest-edge of $t$.*

*b) The 8T-LE partition never partitions a solid angle such that, each one of the three associated planar angles is non-obtuse and different from the largest angle of the corresponding triangular face.*

*c) Over each triangular obtuse face $F$ of any tetrahedron $t$, the iterative 8T-LE partition of $t$ produces a finite number of different faces, such that each new face produced is better than the preceding one in the sense that the smallest angle and the largest angle of the new face are respectively greater than and less than those corresponding to the preceding face generated in the preceding iteration.*

*d) Property c) extends to each new obtuse face produced throughout the 8T-LE refinement process (self corrective behavior).*

The theorem proof is essentially based on the 2-dimensional properties of the 4T-LE refinement (Theorem 2.2).

**Theorem 5.3** *(Fractal behavior) For any conforming tetrahedral mesh $\tau_0$, after a finite number of local 3D-Skeleton refinements around any vertex $P$, a finite number of tetrahedra sharing vertex $P$ is obtained whose associated solid angles are never refined again as the refinement around $P$ proceeds.*

At this point some remarks are in order:

1. Part (b) of Theorem 5.2 implies that whenever a solid angle having non-obtuse planar angles (each one not opposite to the longest-edge of the corresponding triangular face) is obtained throughout the process, this solid angle remains untouched forever in the mesh. In other words, only new vertices along the edges of this solid angle are added as the refinement proceeds.

2. Parts (c) and (d) of Theorem 5.2 together state that the strong quality improvement properties of the 2-dimensional 4-Triangles partition hold over each triangular face of the 2D-Skeleton mesh, including the new faces.

3. Theorems 5.2 and 5.3 together do not certainly guarantee that the size of the molecules (set of tetrahedra sharing a given vertex of the mesh) do not increase as new vertices are added in the refinement process. However, empirical experimentation shows that a rather constant standard deviation around the average size of the molecules is obtained through the refinement steps, while the maximum size of them remains rather constant (equal to 64) in the last three levels.

## 6. EMPIRICAL RESULTS

In this section we report empirical evidence that supports the conjecture on the non-degeneracy property of both the 8T-LE partition and the mesh refinement algorithms based on this partition.

Here three numerical examples are presented. In every case the 8T-LE partition has been applied 7 times to an initial tetrahedron and its descendants, so the last level of division ($\tau_8$) contains $366,145$ vertices and $2,097,152$ tetrahedra. For each test tetrahedron a set of 3 tables have been produced: the first one contains the coordinates of the vertices, while that the second and third ones summarize statistical information for the meshes obtained. The values $\Phi_T, \Phi_{min}$ and $\Phi_{max}$ expressed in sexagesimal degrees, refer to the solid angle measure ($\Phi_P = \sin^{-1}\{(1 - \cos^2\alpha_P - \cos^2\beta_P - \cos^2\gamma_P + 2\cos\alpha_P\cos\beta_P\cos\gamma_P)^{1/2}\}$, where $\alpha_P$, $\beta_P$, $\gamma_P$ are the planar angles associated to vertx $P$) used by Rivara and Levin [18], where $\Phi_T$ is the minimum $\Phi$-value for the solid angles of tetrahedron $T$, and $\Phi_{min}$ and $\Phi_{max}$ are respectively equal to the minimum and maximum $\Phi$-values attained for the mesh at level $n$. Note that $0 \leqslant \Phi_T \leqslant 45^\circ$ and $\Phi = 0$ implies a totally degenerate tetrahedron. For a discussion on tetrahedron shape measures see [5].

It should be pointed out here that the improvement behavior of any tetrahedron $T$ will be in general studied relative to the quality of the tetrahedra of the first volume partition of $T$. This is due to the fact that the quality measures $\Phi_{T_i}$ associated to the tetrahedra $T_i$ ($i = 1, \ldots, 8$), of the first partition of a tetrahedron $T$, in general describe better the local feature sizes of $T$ than the $\Phi_T$ measure itself. Consider for instance a cap (very flat) tetrahedron having four quality acceptable faces which clearly do not reflect well the tetrahedron quality; the first 8-tetrahedra partition of $T$ in exchange, introduces at least a bad quality face that describe well the thickness of $T$.

**Table 1**: Right-tetrahedron vertices

| | | |
|---|---|---|
| 0.0 | 0.0 | 0.0 |
| 4.0 | 0.0 | 0.0 |
| 0.0 | 4.0 | 0.0 |
| 0.0 | 0.0 | 4.0 |

In the first test problem the initial tetrahedron is a right-tetrahedron, with a vertex in the origin of the coordinate system, and three vertices over the axes of the coordinate system to equal distance from the origin. The evolution of the shape for the tetrahedra as the partition proceeds is shown in Table 5. Note that, as expected, the minimum solid angle remains constant since the second global partition, while the percentage of volume covered by bad-shaped elements decreases monotonically from the third global partition. Figures 8, 9, and 10 show the evolution of the average number of tetrahedra per vertex as the global refinement (partition) proceeds. Note that the distribution seems to tend to a bimodal distribution, with concentrations between 15 and 20, and between 45 and 50, with average around 24, which is the asymptotic average number for this partition. Also the maximum number of tetrahedra per vertex is included in the figures.

The second example considers a needle tetrahedron. Table 6 shows the evolution of the minimum and maximum angles, and the % of volume covered by bad-shaped elements, while Figure 9 shows the evolution of tetrahedra per node for this needle tetrahedron where the distribution also approaches the mean value 24. Note that in this case, since the faces of $T$ reflect well the local feature sizes of this needle tetrahedron, the worst solid angle remains constant throughout the process.

**Table 2**: Needle tetrahedron vertices

| | | |
|---|---|---|
| -0.5 | 0.0 | 0.0 |
| 0.5 | 0.0 | 0.0 |
| 0.0 | 0.2 | 0.0 |
| 0.0 | 0.0 | 7.0 |

The third example corresponds to a flat tetrahedron. Table 7 shows for this example the evolution of the shape of the elements and meshes obtained at global partitioning. Note that the minimum solid angle remains constant from the second global refinement, while the percentage of volume covered by bad-shaped tetrahedra improves when the partitioning proceeds.

**Table 3**: Flat tetrahedron vertices

| | | |
|---|---|---|
| -2.0 | 0.0 | 0.0 |
| 4.0 | 0.0 | 0.0 |
| 1.3 | 3.5 | 0.0 |
| 1.0 | 1.3 | 0.5 |

Finally, Table 4 shows the evolution of the average number of tetrahedra per vertex in the first 10 steps of global iterative application of the 8T-LE partition to any initial tetrahedron.

It should be pointed out here that the 3D partition seems to have similar behavior to the 2D case in the sense that for needle tetrahedra (equivalent to one small-angled triangle), a clear monotonic improvement behavior holds, while that for quality tetrahedra and cap tetrahedra a limited decreasing of the tetrahedron quality can be observed in the first partition. Note that in 2-dimensions, the 4-triangles partition of an equilateral triangle produces some 30 degrees triangles, and this is the only case where the bound in part (2) of Theorem 2.1 is attained. For the cap tetrahedron in exchange, the first 3D partition introduces an acute face that captures the thickness of this tetrahedron (a local feature size not described by its four faces). Note that this is not the case of a needle tetrahedron where its faces fully describe its local feature sizes.

**Table 4**: Statistical Measures

| Level | Num. Tets. | $Av\#$(tets per node) |
|---|---|---|
| 4 | 512 | 12.41 |
| 5 | 4,096 | 16.90 |
| 6 | 32,768 | 20.03 |
| 7 | 262,144 | 21.88 |
| 8 | 2,097,152 | 22.91 |
| 9 | 16,777,216 | 23.45 |
| 10 | 134,217,728 | 23.72 |
| 11 | 1,073,741,824 | 23.86 |
| 12 | 8,589,934,592 | 23.93 |
| 13 | 68,719,476,736 | 23.96 |

## 7. CONCLUDING REMARKS

Although in the last 15 years the longest-edge refinement algorithms have become well-known and useful techniques which guarantee the construction of quality refined meshes in 2-dimensions, equivalent non-degeneracy properties had not been proved yet in 3-dimensions. The question was essentially centered before either on finding a lower bound on the minimum solid angle or on looking for results on the number of similarly distinct tetrahedra produced. This last approach is a rather difficult path to follow because of the combinatorial issues involved in 3-dimensions.

In this paper we see that stronger improvement and fractal properties proved for 2-dimensional longest-edge based algorithms [17], also hold over the triangular faces of the volume meshes. The use of these properties seems to be a fruitful path for obtaining mathematical results on the 3-dimensional longest-edge algorithms.

This paper include theoretical and empirical results on this direction: We have discussed a longest-edge based volume algorithm which induces the 4-Triangles partition of the faces of the tetrahedra. The improvement and fractal properties of the 4-Triangles longest-edge partition have been in turn used to prove statistical and fractal properties over the 8-Tetrahedra longest-edge refinement algorithm: (1) the asymptotic average number of tetrahedra surrounding each vertex is equal to 24; (2) the number of tetrahedra surrounding each fixed vertex remains constant, after a few local iterative refinement around such a vertex; and (3) the algorithm improves each triangular face produced as the refinement proceeds.

Empirical study carried out here not only supports these results but also shows that, consistently throughout the refinement levels the distribution of quality tetrahedra improve and the volume percentage covered by better tetrahedra increase as the refinement proceeds.

**Table 5**: Shape evolution for a right-tetrahedron

| *Level* | *Num. of Nodes* | *Num. of Elems.* | $\Phi_{min}$ | *Planar angles associated to* $\Phi_{min}$ | $\Phi_{max}$ | *% bad elems.* ($\Phi_T < 10$) |
|---|---|---|---|---|---|---|
| 1 | 4 | 1 | 30.00 | 45.00 # 60.00 # 45.00 | 90 | 0.00 |
| 2 | 10 | 8 | 9.59 | 19.47 #35.26 # 30.00 | 90 | 25.00 |
| 3 | 35 | 64 | 9.59 | 30.00 #35.26 # 19.47 | 90 | 25.00 |
| 4 | 165 | 512 | 9.59 | 30.00 #35.26 # 19.47 | 90 | 20.31 |
| 5 | 969 | 4096 | 9.59 | 30.00 #35.26 # 19.47 | 90 | 15.62 |
| 6 | 6545 | 32768 | 9.59 | 30.00 #35.26 # 19.47 | 90 | 11.82 |
| 7 | 47905 | 262144 | 9.59 | 30.00 #35.26 # 19.47 | 90 | 8.89 |
| 8 | 366145 | 2097152 | 9.59 | 30.00 #35.26 # 19.47 | 90 | 6.67 |

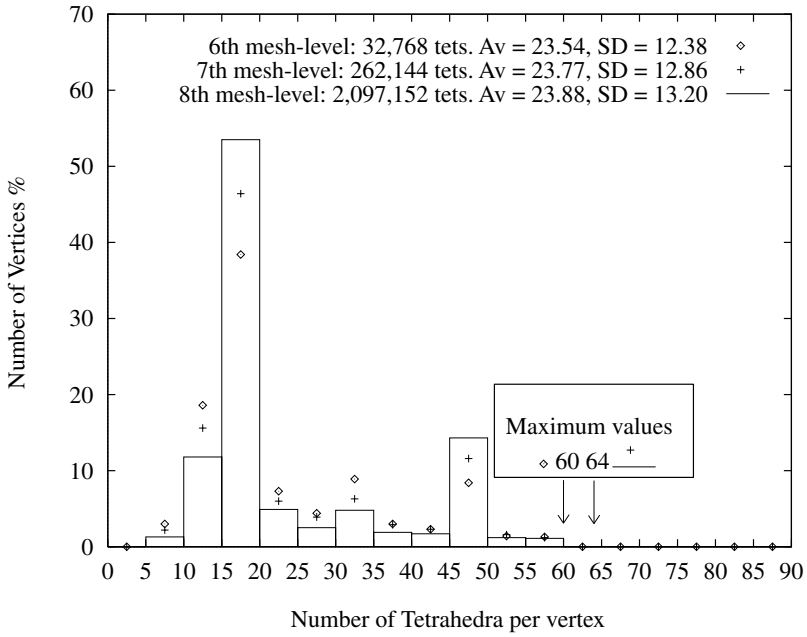


**Figure 8**: Distribution of vertices versus number of tetrahedra per vertex. Right-Shaped Tetrahedron.

**Table 6**: Shape evolution for a needle tetrahedron.

| *Level* | *Num. of Nodes* | *Num. of Elems.* | $\Phi_{min}$ | *Planar angles associated to* $\Phi_{min}$ | $\Phi_{max}$ | *% bad elems.* ($\Phi_T < 0.24$) |
|---|---|---|---|---|---|---|
| 1 | 4 | 1 | 0.23 | 8.00 # 4.36 # 4.28 | 43.58 | 100.00 |
| 2 | 10 | 8 | 0.23 | 8.00 # 4.26 # 4.28 | 67.84 | 75.00 |
| 3 | 35 | 64 | 0.22 | 4.26 # 4.36 # 8.00 | 68.14 | 68.75 |
| 4 | 165 | 512 | 0.22 | 4.28 # 4.36 # 8.01 | 68.14 | 67.19 |
| 5 | 969 | 4096 | 0.22 | 4.23 # 4.35 # 7.96 | 68.14 | 66.80 |
| 6 | 6545 | 32768 | 0.22 | 4.23 # 4.35 # 7.96 | 68.14 | 66.71 |
| 7 | 47905 | 262144 | 0.22 | 7.96 # 4.23 # 4.35 | 68.14 | 66.63 |
| 8 | 366145 | 2097152 | 0.22 | 7.96 # 4.23 # 4.35 | 68.14 | 66.63 |

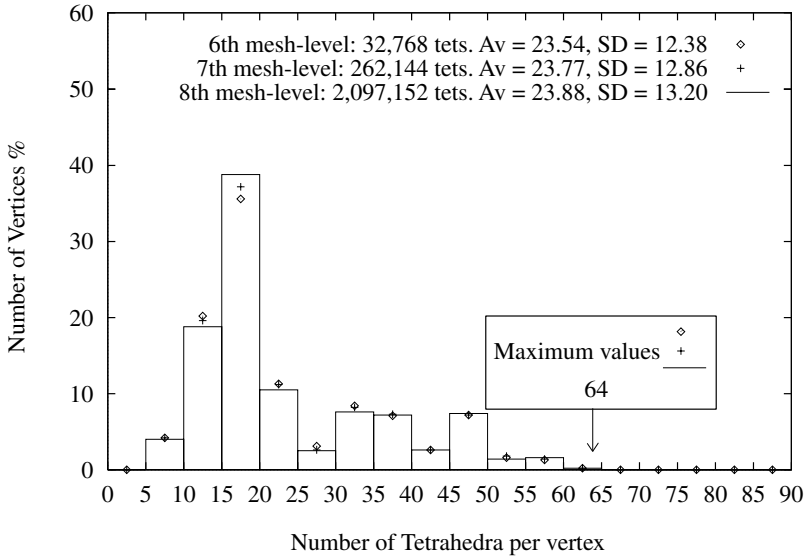


**Figure 9**: Distribution of vertices versus number of tetrahedra per vertex. Needle Tetrahedron.

**Table 7**: Shape evolution for a flat tetrahedron.

| *Level* | *Num. of Nodes* | *Num. of Elems.* | $\Phi_{min}$ | *Planar angles associated to* $\Phi_{min}$ | $\Phi_{max}$ | *% bad elems.* ($\Phi_T < 10$) |
|---|---|---|---|---|---|---|
| 1 | 4 | 1 | 6.31 | 24.90 # 24.74 # 46.78 | 24.94 | 100.00 |
| 2 | 10 | 8 | 3.68 | 40.11 # 6.08 # 38.42 | 33.30 | 62.50 |
| 3 | 35 | 64 | 3.12 | 46.68 # 27.74 # 19.70 | 75.29 | 45.31 |
| 4 | 165 | 512 | 3.12 | 46.68 # 27.74 # 19.70 | 75.29 | 37.50 |
| 5 | 969 | 4096 | 3.12 | 46.68 # 27.74 # 19.70 | 75.29 | 30.03 |
| 6 | 6545 | 32768 | 3.12 | 46.68 #27.74 #19.70 | 75.29 | 22.97 |
| 7 | 47905 | 262144 | 3.12 | 46.68 # 27.74# 19.70 | 75.29 | 17.13 |
| 8 | 366145 | 2097152 | 3.12 | 19.70#46.78# 27.74 | 74.85 | 12.57 |

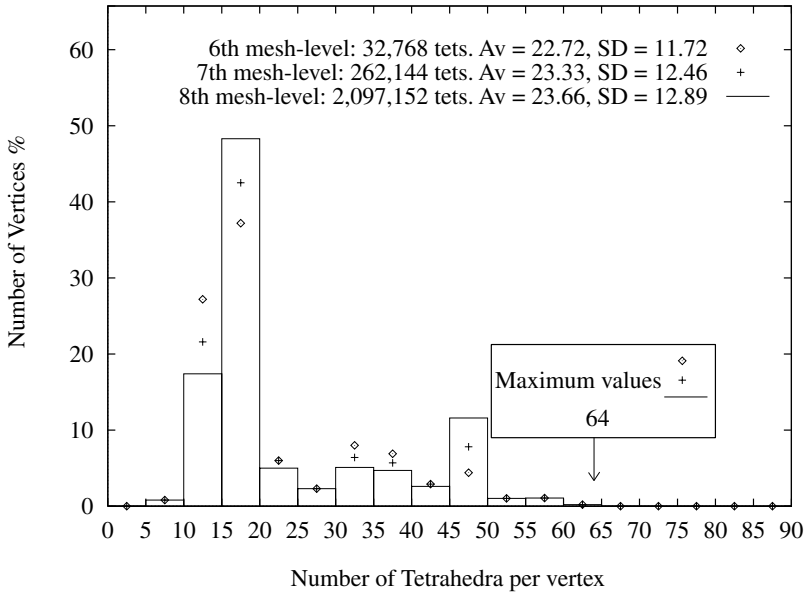


**Figure 10**: Distribution of vertices versus number of tetrahedra per vertex. Flat Tetrahedron.

## References


[1] Arnold D.N., Mukherjee A., Pouly L. "Locally adapted tetrahedra meshes using bisection." *SIAM J. Sci. Comp.*, vol. 22 (2), 431–448, 2001

[2] Bänsch E. "Local Mesh Refinement in 2 and 3 Dimensions." *IMPACT Comp. Sci. Eng.*, vol. 3, 181–191, 1991

[3] Berger M. *Geometry.* Springer-Verlag, Berlin, 1987

[4] Kosaczký I. "A recursive approach to local mesh refinement in two and three dimensions." *J. Compt. Appl. Math.*, vol. 55, 275–288, 1994

[5] Liu A., Joe B. "Relationship between tetrahedron shape measures." *BIT*, vol. 34, 268–287, 1994

[6] Liu A., Joe B. "On the shape of tetrahedra from bisection." *Mathematics of Computation*, vol. 63, no. 207, 141–154, 1994

[7] Liu A., Joe B. "Quality local refinement of tetrahedral meshes based on bisection." *SIAM J. Sci. Compt.*, vol. 16, 1269–1291, 1995

[8] Maubach J.M. "Local bisection refinement for $n$-simplicial grids generated by reflection." *SIAM J. Sci. Compt.*, vol. 16, 210–227, 1995

[9] Mitchell W.F. "Optimal multilevel iterative methods for adaptive grids." *SIAM J. Sci. Stat. Comput.*, vol. 13, 146–167, 1992

[10] Plaza A., Carey G.F. "About local refinement of tetrahedral grids based on bisection." *Proceedings* $5^{th}$ *Int. Meshing Roundtable*, pp. 123–136. 1996

[11] Plaza A., Carey G.F. "Refinement of simplicial grids based on the skeleton." *Appl. Numer. Math.*, vol. 32 (2), 195–218, 2000

[12] Plaza A., Padrón M.A., Carey G.F. "A 3D refinement/derefinement algorithm for solving evolution problems." *Appl. Numer. Math.*, vol. 32 (4), 401–418, 2000

[13] Plaza A., Rivara M.C. "On the adjacencies for triangular meshes based on skeleton-regular partitions." *J. Compt. Appl. Math.*, vol. 140 (1-2), 673–693, 2002

[14] Rivara M.C. "Algorithms for Refining Triangular Grids Suitable for Adaptive and Multigrid Techniques." *Int. J. Num. Meth. Eng.*, vol. 20, 745–756, 1984

[15] Rivara M.C. "Selective Refinement/Derefinement Algorithms for Sequences Nested Triangulations." *Int. J. Num. Meth. Eng.*, vol. 28, 2889–2906, 1989

[16] Rivara M.C. "New longest-edge algorithm for the refinement and/or improvement of unstructured triangulations." *Int. J. Num. Meth. Eng.*, vol. 40, 3313–3324, 1997

[17] Rivara M.C., Iribarren G. "The 4-Triangles Longest-Side Partition and Linear Refinement Algorithms." *Math. Comp.*, vol. 65, 1485–1502, 1996

[18] Rivara M.C., Levin C. "A 3D Refinement Algorithm Suitable for Adaptive and Multigrid Techniques." *Comm. Appl. Num. Meth.*, vol. 8, 281–290, 1992